Available online at http://scik.org

J. Math. Comput. Sci. 10 (2020), No. 4, 758-777

https://doi.org/10.28919/jmcs/4347

ISSN: 1927-5307

THE EFFECT OF A STEP CHANGE IN SEABED DEPTH ON SPREADING DISCHARGED BRINE EFFLUENTS FROM A TWO-OUTFALL SYSTEM

ANTON PURNAMA*, HUDA A. AL-MAAMARI, ABDULLRAHMAN A. AL-MUQBALI,

AND E. BALAKRISHNAN

Department of Mathematics, College of Science, PO Box 36, Sultan Qaboos University, Al-Khod PC 123,

Muscat, Sultanate of Oman

Abstract: Discharged brine effluents from coastal desalination plants through marine outfall systems contain some reactive chemicals that may be derived from corrosion product, toxic antifoulants, antiscalants and other chemicals used in desalinating seawater. These effluents are subject to significant loss due to temporal decay that varies with water depth as the results of consumption by bacteria or radioactive decay, heat loss or evaporation through the surface, and break up or dissolution by turbulence. A far-field model using a two-dimensional decay-advection-diffusion equation with two point sources in a simple step seabed profile is presented to study the variability of decay with water depth. Analytical solutions are illustrated graphically by plotting contours of concentration to simulate the spreading of discharged brine effluent plumes from two outfalls in coastal waters. The maximum value of the compounded concentration at the shoreline is formulated and used as a measure for assessing the quality standards of coastal waters. It is found that, for coastal effluent discharges, the modern engineering practice which installs a two-port diffuser at the end of the outfall pipeline does produce low potential environmental impact.

Keywords: decay-advection-diffusion equation; method of image; shoreline concentration; two-port diffuser.

2010 AMS Subject Classification: 35Q99, 76R99.

---

*Corresponding author

E-mail address: antonp@squ.edu.om

Received October 24, 2019

1. INTRODUCTION

An outfall is a long pipeline which terminates in a diffuser that continuously discharges large amounts of (treated) municipal wastewaters, cooling waters, or desalination brine effluents into the open sea [1,2,3,4,5]. In some situations, where the coastal plant's capacity is expanding, a second outfall may need to be built nearby the first outfall [6,7,8]. Brine effluents from coastal desalination plants contain some unknown reactive chemicals use in desalinating seawater that are subject to significant temporal decay that varies with water depth. During the plants maintenance, these brine effluents may consist of corrosion product, toxic antifoulants and antiscalants [5,9,10]. In the coastal waters, the decay processes [2,4,11,12,13] include consumption by bacteria or radioactive decay (temporal decay uniform across the flow), heat loss or evaporation through the surface (decay decreasing with depth), and break up or dissolution by turbulence (decay proportional to the velocity). For calm sea conditions, the time scales for transverse mixing can be of order a day and comparable with the time scales for decay. So, the effects of decay can not be regarded as a minor perturbation that simply lowers the concentration of discharged effluents.

If these discharges of brine effluent into the sea cannot be avoided, then it should be done as optimally as possible to ensure that the environmental impact is minimized and that public health is protected for using the beaches for swimming and other recreational purposes. It is observed in the far-field that the discharged effluent plumes are spreading towards the coastline and may impair the quality of coastal waters and affect marine life [1,2,5,8]. One factor affecting the dispersion of wastewater effluents is the seabed depth profiles [7,14,15], which typically range between a sloping sandy beach and a mountainous coast with rocky coastal cliffs, where the water depth gets very deep within a short distance from the coastline.

Mathematical modeling has been widely used to demonstrate the effectiveness of an outfall with minimal environmental impacts [16,17,18]. Far-field model studies of the effect of the seabed depth profile on spreading brine effluent discharges in the coastal waters is investigated using a two-dimensional decay-advection-diffusion equation with two point sources. Some beach profiles are extremely flat where variations in water depth become insignificant. Therefore, we introduce a simple step seabed depth profile to account for the effect of a sharp depth changes across the line $y = \ell h_0$ (parallel to the straight shoreline at $y = 0$) on spreading effluent discharges in the coastal waters (Figure 1 left). h_0 is the water depth in the (finite) nearshore region $0 \le y < \ell h_0$ and h_1 the water depth in the (semi-infinite) offshore region $y > \ell h_0$, where $r = h_1/h_0$. Note that if $r = 1$ and/or $\ell = 0$, there is no depth change, and this depth profile represents a highly simplify flat seabed.

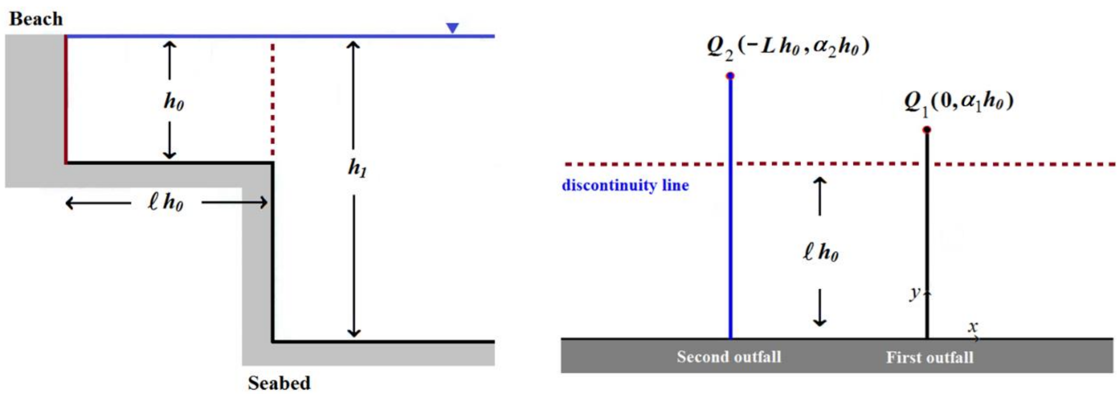

Figure 1. Cross-section depth profile of a step seabed (left); and Plan view of two point sources in a step seabed (right)

The shoreline is assumed to be straight, and as illustrated on Figure 1 (right), we consider two outfalls at Lh_0 distance apart, and each outfall is sufficiently long so that the discharged brine effluent plumes do not feel the presence of the (vertical) shoreline at $y = 0$. The first outfall of length $\alpha_1 > \ell$ is represented as a point source located at $(x = 0, y = \alpha_1 h_0)$ discharging brine effluent at a rate Q_1. Similarly, we represent the second outfall of length $\alpha_2 > \alpha_1$ as a second point source at $(x = -Lh_0, y = \alpha_2 h_0)$ discharging at a different rate Q_2. We also assume that the discharged effluent plume in the far-field is vertically well-mixed over the water depth. Note that, for the case of two outfalls operated by one plant, a combined total rate of discharged brine effluent $Q = Q_1 + Q_2$.

The longshore (drift) current in the shallow nearshore region is assumed to be steady with speed U_0 and remain in the *x*-direction (positive to the right of the discharge point). The dispersion processes are represented by eddy diffusivities D_0, and diffusion in the *x*-direction is neglected, as the effluent plumes in steady currents become very elongated in the direction parallel to the beach. For applications, we take U_0 to be proportional to $h_0^{1/2}$ and D_0 to $h_0^{3/2}$. These scalings are appropriate for a turbulent shallow-water flow over a smooth bed [14,15,19]. In the deeper offshore region, we model both the current U_1 and coefficient of dispersivity D_1 as the power functions of water depth, where U_1 is proportional to $h_1^{1/2}$ and D_1 to $h_1^{3/2}$. The (first-reaction) temporal decay rate is represented by μ_0, and since there are no information available on brine effluent decay rate, we use a typical value up to 0.5 day^{-1} for decay of faecal in recreation coastal waters [20], decay of dissolved oil (biological consumption of hydrocarbons) [21], and decay of biological oxygen demand [22]. Also, we assume that the loss rate μ_1 as a function of water depth and proportional to $h^{1/2+\sigma}$ [12,13], and thus, $\mu_1 = \mu_0 r^{1/2+\sigma}$. In the far-field modeling [16,17], the other complexities such as tidal motions, density and temperature are omitted.

On writing the concentration of discharged brine effluents as

$$c(x,y) = \begin{cases} c_{0*}(x,y), & 0 \le y < \ell h_0 \\ c_{1*}(x,y), & y > \ell h_0 \end{cases},$$

the analytical solution of the decay-advection-diffusion equation with two point sources in a step seabed can be obtained using the method of images, where the depth discontinuity at the line $y = \ell h_0$ will be considered as a reflecting or absorbing barrier. For example, as illustrated in Figure 2 (right), for each (actual) point source located in the offshore region, an observer (in the offshore region) will supposedly see this source plus its own image source on the other side of the reflecting barrier at $y = \ell h_0$ [15]. However, for an observer in the nearshore region, he or she will see one associated virtual (instead of the actual) source over the absorbing barrier at $y=\ell h_0$ (Figure 2 left).

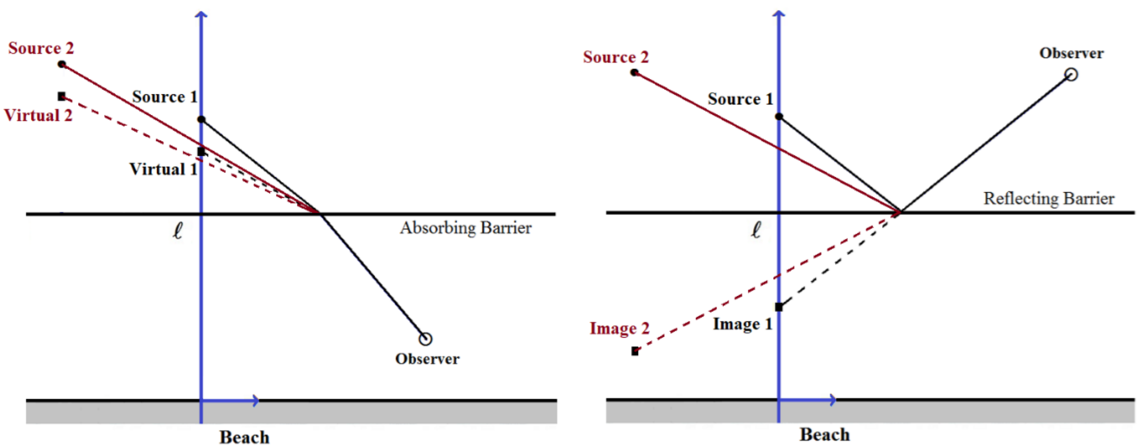

Figure 2. The method of images for two point sources located in the deeper region in a step seabed

2. Decay-Advection-Diffusion Equation with Two Point Sources

Since we are interested in sufficiently long sea outfalls, we consider two point sources located in the offshore region $y>\ell h_0$ (Figure 2). By treating the discontinuity line $y=\ell h_0$ as an absorbing barrier, the concentration $c_{0*}(x,y)$ in the nearshore region $0\le y<\ell h_0$ is obtained from two virtual sources at $(x=0, y=\beta_1 h_0)$ and $(x=-Lh_0, y=\beta_2 h_0)$ discharging with a rate bQ_1 and bQ_2, respectively. Applying the superposition principle, the decay-advection-diffusion equation for $c_{0*}(x,y)$ is given by

$$h_0\mu_0 c_{0*}+h_0U_0\frac{\partial c_{0*}}{\partial x}-h_0D_0\frac{\partial^2 c_{0*}}{\partial y^2}=bQ_1\,\delta(x)\delta(y-\beta_1 h_0)+bQ_2\,\delta(x+Lh_0)\delta(y-\beta_2 h_0), \quad (1)$$

with the boundary condition $h_0D_0\,\partial c_{0*}/\partial y=0$ at the shoreline $y=0$, where $\delta(*)$ is the Dirac delta function which represents the position of a (virtual) point source. The temporal decay term can be eliminated from equation (1) by re-writing

$$c_{0*} = c_0 \exp\left(-\frac{\mu_0 x}{U_0}\right).$$

Note that the concentration of discharged effluents at the shoreline can be adjusted by varying the outfall's length. Thus, for a sufficiently long sea outfall, the boundary condition at the shoreline is conveniently satisfied.

For graphical representation of the solution, we introduce the following dimensionless quantities

$$y = Y h_0, \;\; x = X h_0, \;\; \lambda = \frac{U_0 h_0}{D_0}, \;\; \gamma = \frac{\mu_0 h_0}{U_0} \;\; \text{and} \;\; c_{0,1}(x, y) = \frac{C_{0,1}(X, Y)Q}{h_0{}^2 U_0}.$$

In dimensionless form,

$$C_{0*}(X, Y) = C_0\left[\exp(-\gamma X) + \exp\{-\gamma(X + L)\}\right]$$

and thus, equation (1) is reduced to

$$\frac{\partial C_0}{\partial X} - \frac{1}{\lambda}\frac{\partial^2 C_0}{\partial Y^2} = bq_1\,\delta(X)\delta(Y - \beta_1) + bq_2\,\delta(X + L)\delta(Y - \beta_2),$$

and for $X \geq -L$, the analytical solution is given by

$$C_0 = bq_1\sqrt{\frac{\lambda}{4\pi X}}\exp\left\{-\frac{\lambda(Y - \beta_1)^2}{4X}\right\} + bq_2\sqrt{\frac{\lambda}{4\pi(X + L)}}\exp\left\{-\frac{\lambda(Y - \beta_2)^2}{4(X + L)}\right\}, \qquad (2)$$

where $q_1 = Q_1/Q$, $q_2 = Q_2/Q$ and Q denotes a reference discharge rate which usually adopts the value of the original discharge rate of the first (single) outfall. The model parameter λ represents the discharged effluent plume elongation in the *x*-direction, the larger the values of λ, the more elongated the plumes are, which is mostly due to a stronger current U_0 with less longitudinal dispersivity D_0. The other model parameter γ represents the loss rate of discharged effluents. However, the larger values of γ are mostly due to a stronger decay μ_0 with calm sea conditions U_0. The decay rate is naturally small, and in order for the effects of decay to be noticeable, a sufficiently large values of γ should be considered. For model applications in coastal waters, appropriate values are $\lambda = 0.2$ and $\gamma = 0.0005$.

In the offshore region $y > \ell h_0$, the discontinuity line $y = \ell h_0$ is treated as a reflecting barrier (Figure 2), and the concentration $c_{1*}(x, y)$ is obtained due to the first (actual) source at $(x = 0, y = \alpha_1 h_0)$ discharging at rate Q_1 and due to an image source at $(x = 0, y = (2\ell - \alpha_1)h_0)$ discharging at different rate aQ_1; and the second (actual) source at $(x = -Lh_0, y = \alpha_2 h_0)$ discharging at rate Q_2 and due to an image source at $(x = -Lh_0, y = (2\ell - \alpha_2)h_0)$ discharging at different rate aQ_2. Thus, the decay-advection-diffusion equation for $c_{1*}(x, y)$ is

$$\begin{aligned} h_1\mu_1 c_{1*} + h_1 U_1 \frac{\partial c_{1*}}{\partial x} - h_1 D_1 \frac{\partial^2 c_{1*}}{\partial y^2} &= Q_1\delta(x)\delta(y - \alpha_1 h_0) + aQ_1\delta(x)\delta(y - 2\ell h_0 + \alpha_1 h_0) + \\ &\quad Q_2\delta(x + Lh_0)\delta(y - \alpha_2 h_0) + aQ_2\delta(x + Lh_0)\delta(y - 2\ell h_0 + \alpha_2 h_0) \end{aligned}, \qquad (3)$$

with the condition $c_{1*}(x, y) \to 0$ as $y \to \infty$, where $U_1 = U_0 r^{1/2}$, $D_1 = D_0 r^{3/2}$ and $\mu_1 = \mu_0 r^{1/2+\sigma}$. Again by writing $c_{1*} = c_1 \exp(-\mu_1 x / U_1)$, which in dimensionless form

$$C_{1*}(X, Y) = C_1\left[\exp(-\gamma r^\sigma X) + \exp\{-\gamma r^\sigma (X + L)\}\right]$$

and (3) becomes

$$\begin{aligned} \frac{\partial C_1}{\partial X} - \frac{r}{\lambda}\frac{\partial^2 C_1}{\partial Y^2} = \frac{1}{r^{3/2}}\big[& q_1\delta(X)\{\delta(Y - \alpha_1) + a\delta(Y - 2\ell + \alpha_1)\} + \\ & q_2\delta(X + L)\{\delta(Y - \alpha_2) + a\delta(Y - 2\ell + \alpha_2)\}\big] \end{aligned}.$$

The analytical solution for $X \ge -L$ can be written as

$$\begin{aligned} C_1 = {} & \frac{q_1}{r^2}\sqrt{\frac{\lambda}{4\pi X}}\left[\exp\left\{-\frac{\lambda(Y - \alpha_1)^2}{4rX}\right\} + a\exp\left\{-\frac{\lambda(Y - 2\ell + \alpha_1)^2}{4rX}\right\}\right] + \\ & \frac{q_2}{r^2}\sqrt{\frac{\lambda}{4\pi(X + L)}}\left[\exp\left\{-\frac{\lambda(Y - \alpha_2)^2}{4r(X + L)}\right\} + a\exp\left\{-\frac{\lambda(Y - 2\ell + \alpha_2)^2}{4r(X + L)}\right\}\right] \end{aligned}. \qquad (4)$$

As there can be no sharp discontinuities in either the concentration or its gradient across the line $y = \ell h_0$, the additional matching conditions

$$\lim_{y \to \ell h_0} c_{0*} = \lim_{y \to \ell h_0} c_{1*} \quad \text{and} \quad \lim_{y \to \ell h_0} h_0 D_0 \frac{\partial c_{0*}}{\partial y} = \lim_{y \to \ell h_0} h_1 D_1 \frac{\partial c_{1*}}{\partial y}$$

are required for calculating a, b and β_1 for the first point source and β_2 for the second point source. After some manipulations and simplifications (in dimensionless form), we obtain

$$a = \frac{r^2 - 1}{r^2 + 1}, \; b \exp(-\gamma X) = \frac{2}{r^2 + 1} \exp(-\gamma r^\sigma X), \; b \exp\{-\gamma (X + L)\} = \frac{2}{r^2 + 1} \exp\{-\gamma r^\sigma (X + L)\},$$

$$\beta_1 = \frac{\alpha_1 - \ell}{\sqrt{r}} + \ell \quad \text{and} \quad \beta_2 = \frac{\alpha_2 - \ell}{\sqrt{r}} + \ell .$$

For the case of no decay ($\gamma = 0$) it is easy to verify $a + b = 1$ and in addition, if there is no depth change across the line $y = \ell h_0$, i.e. $r = 1$, then $a = 0$, $b = 1$, $\beta_1 = \alpha_1$ and $\beta_2 = \alpha_2$ (also for the case when $\ell = 0$, since $r = 1$). For the values of $r > 1$, $0 < a < 1$, $\beta_1 < \alpha_1$ and $\beta_2 < \alpha_2$. One of the objectives of a long sea outfall is to prevent the discharged effluent plumes from reaching coastal areas of human usage. Thus, the appropriate location for assessing the impact of effluents discharge into the sea would be at the shoreline, where the maximum value of the concentration at the shoreline can be used as a measure of how well the discharged effluents are being mixed and diluted in the coastal waters [18,23,24]. By substituting $Y = 0$ into (2), we obtain for $X \geq -L$, the compounded concentration at the shoreline from the two point sources

$$C_{0*} = \frac{2}{r^2 + 1} \left[q_1 \sqrt{\frac{\lambda}{4\pi X}} \exp\left(-\frac{\lambda \beta_1^2}{4X} - \gamma r^\sigma X \right) + q_2 \sqrt{\frac{\lambda}{4\pi (X + L)}} \exp\left\{ -\frac{\lambda \beta_2^2}{4(X + L)} - \gamma r^\sigma (X + L) \right\} \right]. \quad (5)$$

The effects of loss of discharged brine effluents that vary with depth can be investigated according to the values of σ. For model applications, the case of no decay $\gamma = 0$, the values of $\sigma = 0$ (constant decay of $\gamma = 0.0005$) and $\sigma = 1$ (decay that increases with depth) will be used.

3. SINGLE OUTFALL

For model applications, we first consider the simplest case of a single outfall ($L=0$) that terminates in a port to investigate the effect of a step depth change on spreading (chemically active) brine effluents discharge in the far field. Since the total effluent load is released through this single outfall at $\left(x=0, y=\alpha_1 h_0\right)$, in this case $q_1=1$ and $q_2=0$.

The solution for a single outfall's discharge in the shallow nearshore region $0 \leq y < \ell h_0$ is obtained from (2)

$$C_{0s}(X, Y)=\frac{2}{r^2+1}\exp(-\gamma r^{\sigma} X)\sqrt{\frac{\lambda}{4\pi X}}\exp\left\{-\frac{\lambda(Y-\beta_1)^2}{4X}\right\}$$

and in the deeper offshore region $y > \ell h_0$ from (4)

$$C_{1s}(X, Y)=\frac{1}{r^2}\sqrt{\frac{\lambda}{4\pi X}}\exp(-\gamma r^{\sigma} X)\left[\exp\left\{-\frac{\lambda(Y-\alpha_1)^2}{4rX}\right\}+a\exp\left\{-\frac{\lambda(Y-2\ell+\alpha_1)^2}{4rX}\right\}\right].$$

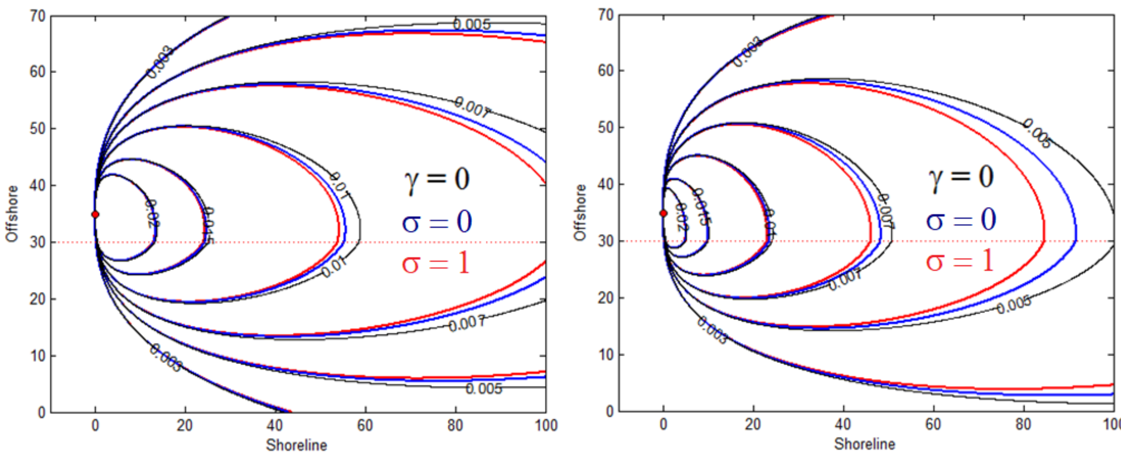

Figure 3. Contours of concentration of discharged effluents from a point source at $\alpha_1=35$ on a step seabed when $\ell=30$ with $\lambda=0.2$: $r=1.5$ (left); and $r=2$ (right). The case of no decay $\gamma=0$ (black contour), constant decay of $\gamma=0.0005$ and $\sigma=0$ (blue contour), and decay that increases with depth $\sigma=1$ and $\gamma=0.0005$ (red contour).

To investigate the effect of a step depth change on spreading discharged effluents, the contour plot of the solutions for a single outfall discharging at $\alpha_1 = 35$ on a step seabed when $\ell = 30$ with $\lambda = 0.2$ is shown in Figure 3 for two different values of depth ratio $r = 1.5$ and $r = 2$. For a small depth ratio (Figure 3 left), it is hard to see the effect of a step depth change across the line $y = \ell h_0$. The plumes spreading toward deeper water can be seen for a large depth ratio $r = 2$ (Figure 3 right), where the offshore water depth is twice that the nearshore depth. Due to loss of effluents, the effluent plumes of $\gamma = 0.0005$ are smaller than that of no decay ($\gamma = 0$) plumes.

The concentration of discharged effluent plumes at the shoreline is obtained from (5)

$$C_{0s}(X,0) = \frac{2}{r^2+1}\sqrt{\frac{\lambda}{4\pi X}}\exp\left(-\frac{\lambda\beta_1^2}{4X} - \gamma r^\sigma X\right).$$

By differentiation, this has a maximum value of

$$C_{sm} = \frac{2}{r^2+1}\sqrt{\frac{\Phi}{4\pi\beta_1^2}}\exp\left(-\frac{\Phi-1}{2}\right),$$

which occurs at

$$X_{sm} = \frac{\lambda\beta_1^2}{\Phi} \quad \text{and} \quad \Phi = 1 + \sqrt{1 + 4r^\sigma\gamma\lambda\beta_1^2}.$$

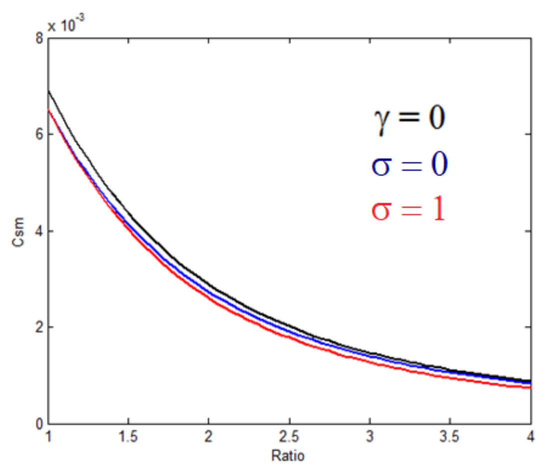

Figure 4. Maximum value of concentration at the shoreline for discharged effluents from a point source at $\alpha_1 = 35$ on a step seabed when $\ell = 30$ with $\lambda = 0.2$. The case of no decay $\gamma = 0$ (black curve), constant decay of $\gamma = 0.0005$ and $\sigma = 0$ (blue curve), and decay that increases with depth $\sigma = 1$ and $\gamma = 0.0005$ (red curve).

For the case of no decay ($\gamma = 0$) it is straightforward to see that $\Phi = 2$, and thus $C_{sm} = 2 / \beta_1 (r^2 + 1) \sqrt{2\pi e}$ and $X_{sm} = \lambda \beta_1^2 / 2$. In addition, if there is no depth change across the line $y = \ell h_0$, i.e. $r = 1$, then $\beta_1 = \alpha_1$. Thus, the maximum value can be adjusted by increasing the value of α_1. The larger the value of α_1, the longer distance travelled for the discharged effluent plumes to reach the shoreline.

This maximum value C_{sm} will be used and served as the base value for the effectiveness design of a two-outfall system. To see the effect of a step depth change, as shown in Figure 4, the value of C_{sm} decreases as the depth ratio *r* increases. For the case of no decay ($\gamma = 0$), C_{sm} decreases from that of $r = 1$ (flat seabed) value of 0.0069 by more than 36% for $r = 1.5$ to less than 58% for $r = 2$. Further, as shown in Table 1, the offshore distance ℓ of the discontinuity line has little effect on the maximum value. Thus, unless stated otherwise, the value of $\ell = 30$ is used in the subsequent calculations and plots. For the case of constant decay of $\gamma = 0.0005$, the maximum values C_{sm} are smaller than that of no decay ($\gamma = 0$) case.

Table 1. Maximum values C_{sm}

no decay	$\ell = 26$			$\ell = 30$			$\ell = 34$		
$\gamma = 0$	$\alpha = 33$	$\alpha = 34$	$\alpha = 35$	$\alpha = 34$	$\alpha = 35$	$\alpha = 36$	$\alpha = 35$	$\alpha = 36$	$\alpha = 37$
$r = 1$	0.0073	0.0071	0.0069	0.0071	0.0069	0.0067	0.0069	0.0067	0.0065
$r = 1.5$	0.0047	0.0046	0.0045	0.0045	0.0044	0.0043	0.0043	0.0042	0.0041
$r = 2$	0.0031	0.0031	0.0030	0.0029	0.0029	0.0028	0.0028	0.0027	0.0027
$r = 2.5$	0.0022	0.0021	0.0021	0.0021	0.0020	0.0020	0.0019	0.0019	0.0019
$r = 3$	0.0016	0.0016	0.0016	0.0015	0.0015	0.0014	0.0014	0.0014	0.0014
$r = 3.5$	0.0012	0.0012	0.0012	0.0011	0.0011	0.0011	0.0011	0.0010	0.0010
$r = 4$	0.0010	0.0009	0.0009	0.0009	0.0009	0.0009	0.0008	0.0008	0.0008

4. Two Independent Outfalls

First we consider the case where the two outfalls are operated independently by two different desalination plants and the value of L is sufficiently large [7,8]. The contours of the concentration solutions (2) and (4) for two outfalls at $\alpha_1 = 35$ and $\alpha_2 = 40$ discharging at equal rate $q_1 = q_2 = 1$ on a step seabed when $\ell = 30$ with $\lambda = 0.2$ are plotted in Figure 5 for two values of $L = 25$ with $r = 1.5$ and $L = 75$ with $r = 2$. These figures graphically illustrate a typical merging discharged effluent plumes from two point sources. For a shorter separation distance $L = 25$ (Figure 5 left), the merging of discharge plumes is more clearer, and for a longer separation distance $L = 75$ (Figure 5 right), it is easy to see two individual discharged plumes. However, downstream of the first outfall (i.e., $X \geq 0$), the combined plumes is spreading like one.

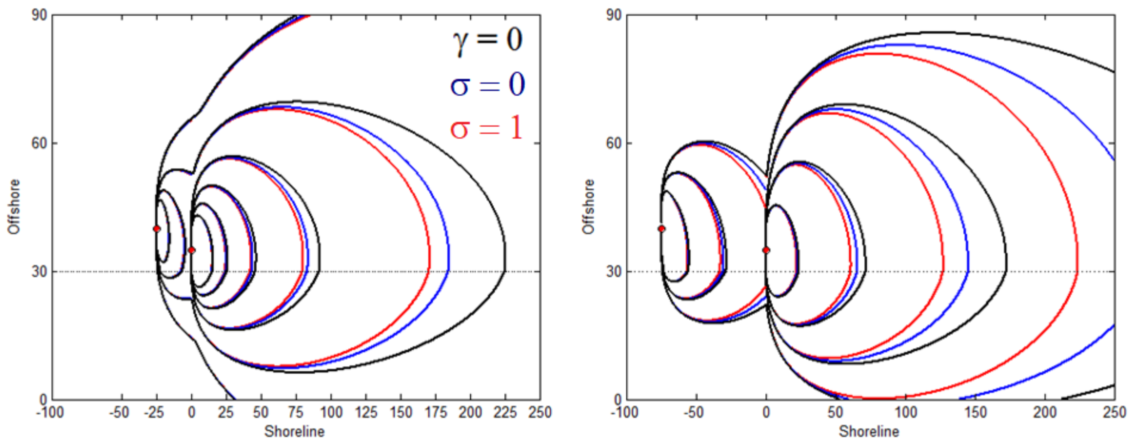

Figure 5. Contours of concentration of discharged effluents from two point sources at $\alpha_1 = 35$ and $\alpha_2 = 40$ on a step seabed when $\ell = 30$ with $\lambda = 0.2$: $L = 25$ and $r = 1.5$ (left); $L = 75$ and $r = 2$ (right). The case of no decay $\gamma = 0$ (black contour), constant decay of $\gamma = 0.0005$ and $\sigma = 0$ (blue contour), and decay that increases with depth $\sigma = 1$ and $\gamma = 0.0005$ (red contour).

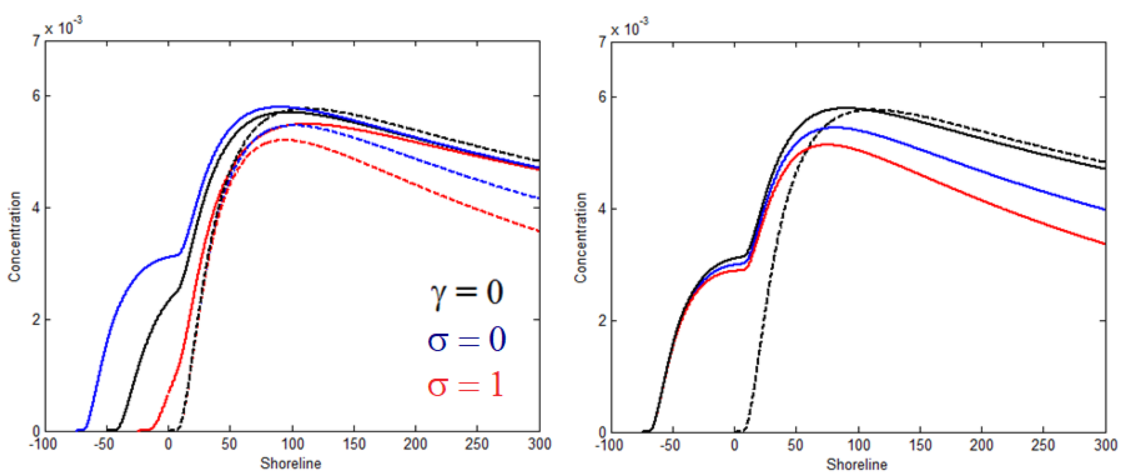

Figure 6. Compounded concentration at the shoreline of discharged effluents when $\ell = 30$ and $r = 2$ with $\lambda = 0.2$

from two point sources at: (left) $\alpha_1 = 35$ and $\alpha_2 = 40$ with $L = 25$ (red curve), $\alpha_1 = \alpha_2 = 35$ with $L_m = 50$ (blue curve), and $\alpha_1 = 35$ and $\alpha_2 = 31$ with $L = 75$ (black curve); (right) $\alpha_1 = 35$ and $\alpha_2 = 31$ with $L = 75$. The case of no decay $\gamma = 0$ (black curve), constant decay of $\gamma = 0.0005$ and $\sigma = 0$ (blue curve), and decay that increases with depth $\sigma = 1$ and $\gamma = 0.0005$ (red curve)

Next, the compounded concentration at the shoreline (5) is shown on Figure 6 for two point sources discharging at equal rate $q_1 = q_2 = 1$ for three values of $L = 25$, 50 and 75. As plotted in Figure 6 (left) for the case of no decay $\gamma = 0$, the two effluent plumes are interacted and merged for the shorter separation distance $L = 25$ (shown in red curve). As the separation distance gets longer, two distinctive concentration peaks are formed (shown in black curve for $L = 50$) and clearly seen (shown in blue curve $L = 75$). For comparison, the concentration at the shoreline for a single outfall at $\alpha_1 = 35$ discharging with a double rate is also shown with a dotted black curve. To account of effluents decay is shown for a constant decay of $\gamma = 0.0005$ and $\sigma = 0$ (blue dotted curve), and decay that increases with depth $\sigma = 1$ and $\gamma = 0.0005$ (red dotted curve).

To investigate the effect of effluents decay on the compounded concentration at the shoreline for two point sources discharging at $\alpha_1 = 35$ and $\alpha_2 = 31$ with $L = 75$ on a step seabed when $\ell = 30$ and $r = 2$ is shown in Figure 6 (right) where $\lambda = 0.2$. For comparison, the concentration at the shoreline for a single outfall at $\alpha_1 = 35$ discharging with a double rate is also shown with a dotted black curve.

Using the single outfall's discharged concentration $C_{0s}(X, 0)$, the compounded concentration at the shoreline (5) simplifies to

$$C_0(X, 0) = C_{0s}(X, 0)\left[q_1 + q_2\sqrt{\frac{X}{X + L}}\exp\left\{-\frac{\lambda\beta_2^2}{4(X + L)} + \frac{\lambda\beta_1^2}{4X} - \gamma r^{\sigma} L\right\}\right].$$

By substituting $X = X_{sm}$, the maximum value can be approximated and written as

$$C_{\max} = C_{sm}\left[q_1 + q_2 \exp\left(\frac{\Phi}{4} - \gamma r^{\sigma} L\right) f(z)\right],$$

where

$$f(z) = \sqrt{\frac{1}{1+z}} \exp\left\{-\frac{\Phi}{4}\left(\frac{\beta_2}{\beta_1}\right)^2 \frac{1}{1+z}\right\} \quad \text{and} \quad z = \frac{L\Phi}{\lambda \beta_1^2}.$$

Thus, since $f_{\max} = (\beta_1/\beta_2)\sqrt{2/e\Phi}$ is the maximum value of $f(z)$ when $\Phi/(1+z) = 2(\beta_1/\beta_2)^2$, the largest value of $C_{\max}$ is simplified to

$$\frac{C_{\max}}{C_{sm}} = q_1 + q_2\left(\frac{\beta_1}{\beta_2}\right)\sqrt{\frac{2}{e\Phi}} \exp\left(\frac{\Phi}{4} - \gamma r^{\sigma} L\right) = q_1 + q_2\left\{\frac{\alpha_1 + \ell(\sqrt{r} - 1)}{\alpha_2 + \ell(\sqrt{r} - 1)}\right\}\sqrt{\frac{2}{e\Phi}} \exp\left(\frac{\Phi}{4} - \gamma r^{\sigma} L\right).$$

Note that the critical separation distance between the outfalls can be determined by $L_m = \lambda(\beta_2^2 - 2\beta_1^2/\Phi)/2$. It is easy to see that $L = 0$ only when $\alpha_2 = \alpha_1$, which represents a single outfall discharging effluents at a double rate of $q_2 + q_1$.

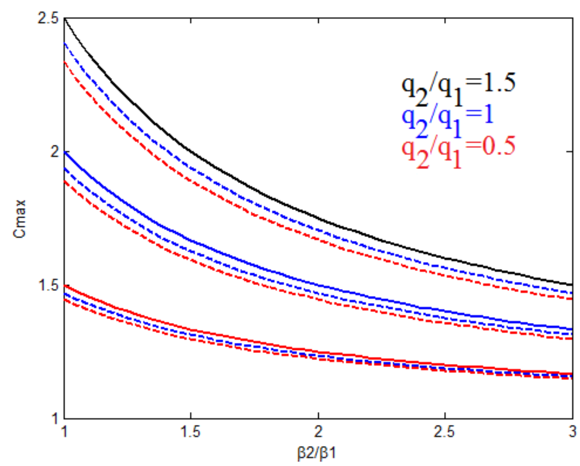

Figure 7. Compounded maximum value $C_{\max}/q_1 C_{sm}$ of discharged effluents from two point sources on a step seabed when $\ell = 30$ and $r = 2$ for $\lambda = 0.2$ and $\alpha_1 = 35$: when $q_2/q_1 = 0.5$ (red curve), $q_2/q_1 = 1$ (blue curve), $q_2/q_1 = 1.5$ (black curve). The case of constant decay of $\gamma = 0.0005$ and $\sigma = 0$ (blue dotted curve), and decay that increases with depth $\sigma = 1$ and $\gamma = 0.0005$ (red dotted curve)

For no decay ($\gamma = 0$) discharged effluents and $\Phi = 2$, the ratio of $C_{\max}/C_{sm} = q_1 + q_2 \beta_1/\beta_2$.

In addition, if there is no depth change across the line $y = \ell h_0$, i.e. $r = 1$, $\beta_1 = \alpha_1$ and $\beta_2 = \alpha_2$ then $C_{\max}/C_{sm} = q_1 + q_2 \alpha_1/\alpha_2$ and $L_m = \lambda(\alpha_2^2 - \alpha_1^2)/2$. For a special case of $\alpha_2 = 2\alpha_1$, then $C_{\max}/C_{sm} = q_1 + q_2/2$. That is, if both outfalls are discharging at an equal rate $q_2 = q_1$, then the maximum value $C_{\max}$ is 50% higher than that of the first outfall $q_1 C_{sm}$. However, if $q_2 = 0.5 q_1$, the maximum value is 25% higher than $q_1 C_{sm}$.

As shown on Figure 7 for three values of $q_2/q_1 = 0.5$, 1 and 1.5, the maximum value of compounded concentration at the shoreline $C_{\max}/q_1 C_{sm}$ decreases as the ratio β_2/β_1 increases. That is, the contribution of the second outfall is smaller if its length α_2 is longer than α_1 and its discharge rate q_2 is smaller than that of the first outfall q_1. Due to decay of discharged effluents, the maximum value $C_{\max}/q_1 C_{sm}$ is smaller than that of no decay ($\gamma = 0$) discharged effluents value.

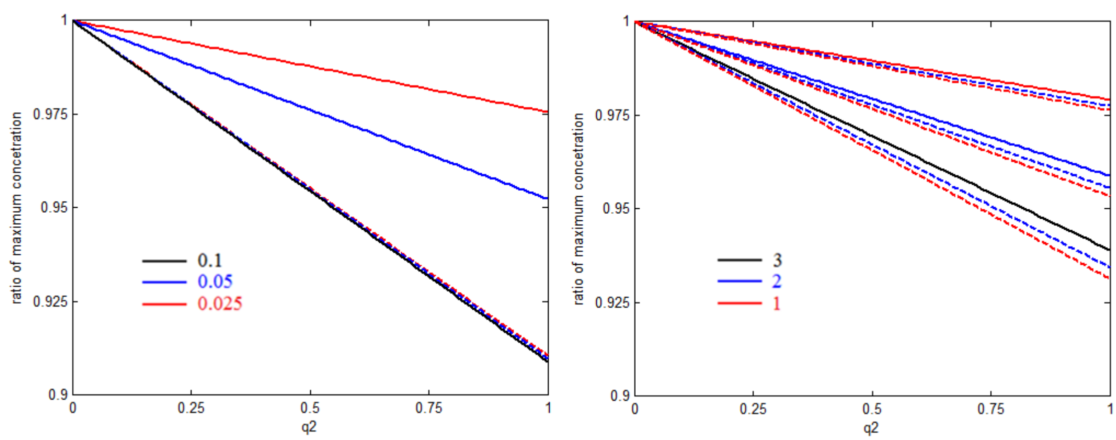

Figure 8. Compounded maximum value $C_{\max}/C_{sm}$ for discharged effluents on a step seabed when $\ell = 30$ and $r = 2$ with $\lambda = 0.2$: (left) two outfalls operated by one plant with $\alpha_1 = 35$ and $\varepsilon/\beta_1\sqrt{r} = 0.025$ (red line), $\varepsilon/\beta_1\sqrt{r} = 0.05$ (blue line) and $\varepsilon/\beta_1\sqrt{r} = 0.1$ (black line). The case of constant decay of $\gamma = 0.0005$ and $\sigma = 0$ (blue dotted line), and decay that increases with depth $\sigma = 1$ and $\gamma = 0.0005$ (red dotted line); (right) a two-port

diffuser with $\alpha_1 = 35$ and $L = 1$: $\varepsilon = 1$ (red line), $\varepsilon = 2$ (blue line) and $\varepsilon = 3$ (black line)

5. TWO OUTFALLS OPERATED BY ONE PLANT

Distributing the brine effluents load between the outfalls is relatively less expensive than extending the lengths of the outfall pipe. If the two outfalls are operated by one plant where the separation distance is not very large $L < L_m$, then the total brine effluent discharges can be shared between them, i.e. $q_2 + q_1 = 1$. On writing $\alpha_2 = \alpha_1 + \varepsilon$, gives $\beta_2 = \beta_1 + \varepsilon/\sqrt{r}$. Assuming $\varepsilon/\beta_1\sqrt{r} < 1$, the binomial expansion gives

$$\frac{\beta_1}{\beta_2} = \left(1 + \frac{\varepsilon}{\beta_1\sqrt{r}}\right)^{-1} = 1 - \frac{\varepsilon}{\beta_1\sqrt{r}} + \left(\frac{\varepsilon}{\beta_1\sqrt{r}}\right)^2 - \left(\frac{\varepsilon}{\beta_1\sqrt{r}}\right)^3 + \cdots.$$

Thus, the maximum value of (5) can be approximated further as

$$\frac{C_{\max}}{C_{sm}} = 1 - q_2\sqrt{\frac{2}{e\Phi}}\exp\left(\frac{\Phi}{4} - \gamma r\sigma L\right)\left\{\frac{\varepsilon}{\beta_1\sqrt{r}} - \left(\frac{\varepsilon}{\beta_1\sqrt{r}}\right)^2 + \cdots\right\}.$$

Note that for the case of no decay ($\gamma = 0$) discharged effluents, and $\Phi = 2$, then the maximum value $C_{\max}/C_{sm} = q_1 + q_2/\left(1 + \varepsilon/\beta_1\sqrt{r}\right)$. In addition, if there is no depth change $r = 1$ and $\beta_1 = \alpha_1$ then $C_{\max}/C_{sm} = 1 - q_2\varepsilon/(\varepsilon + \alpha_1)$. For example, by choosing $\varepsilon/\alpha_1 = 0.1$ then $C_{\max}/C_{sm} = 1 - q_2/11$.

As shown on Figure 8 (left), as the discharge rate q_2 increases and the distance ε gets longer, this value $C_{\max}$ is smaller than that of the maximum value at the shoreline from the first outfall C_{sm}. However, since the value of γ is naturally small, the effect of decay is too small to be noticeable. For example, for no decay ($\gamma = 0$) effluent discharges, if $\varepsilon/\beta_1\sqrt{r} = 0.1$ (or $\varepsilon = 4.74$ for $\ell = 30$ and $r = 2$ with $\alpha_1 = 35$) and the discharge rate q_2 is set at 0.25, then the maximum value $C_{\max}$ is about 2.3% less than C_{sm}. However, if the discharge rate q_2 is increased to 0.75, the maximum value is lowered by 6.8% than that of C_{sm}. This result agrees with the finding that the total effluent load can be optimally allocated between two outfalls to minimize the impact [6,7,8]. However, economically it is cheaper to build just one outfall and install a two-port diffuser at its pipe-end than build two outfalls.

6. OUTFALL WITH A TWO-PORT DIFFUSER

As for the case of the modern engineering practice that installs a two-port diffuser at the end of the outfall pipe, both L and ε are very small in comparison with the first outfall length α_1. After substituting $X = X_{sm}$ and $\beta_2 = \beta_1 + \varepsilon/\sqrt{r}$, the maximum value of compounded concentration at the shoreline can be approximated as

$$\frac{C_{\max}}{C_{sm}} = q_1 + q_2 \exp(-\gamma r \sigma L)\sqrt{\frac{1}{1+z}} \exp\left[-\frac{\Phi}{4}\left\{\left(1+\frac{\varepsilon}{\beta_1\sqrt{r}}\right)^2 \frac{1}{1+z} - 1\right\}\right].$$

Since the value of γ is naturally small and $q_2 + q_1 = 1$, asymptotically we obtain

$$\frac{C_{\max}}{C_{sm}} = 1 - q_2\frac{\Phi}{4}\left[\frac{\varepsilon}{\beta_1\sqrt{r}}\left\{2+\left(1-\frac{\Phi}{2}\right)\frac{\varepsilon}{\beta_1\sqrt{r}} - 3z\right\} + z\left\{\frac{2}{\Phi} - 1 + \left(\frac{3}{2} - \frac{\Phi}{8} - \frac{3}{2\Phi}\right)z\right\}\right] + \cdots.$$

Again, it is easy to see that the maximum value $C_{\max}$ is smaller than that of the first outfall value C_{sm}. For a special design of two-port in a horizontal diffuser line, i.e. $\alpha_2 = \alpha_1$ and $\varepsilon = 0$, then

$$\frac{C_{\max}}{C_{sm}} = 1 - q_2\frac{L}{\lambda\beta_1^2}\frac{\Phi}{4}\left\{2 - \Phi + \left(\frac{12\Phi^2 - \Phi^3 - 12\Phi}{8}\right)\frac{L}{\lambda\beta_1^2} + \cdots\right\}.$$

Similarly, for two-port in a vertical diffuser line, i.e. $L = 0$ and $z = 0$, then

$$\frac{C_{\max}}{C_{sm}} = 1 - q_2\frac{\varepsilon}{\beta_1\sqrt{r}}\frac{\Phi}{2}\left\{1 + \left(\frac{2-\Phi}{4}\right)\frac{\varepsilon}{\beta_1\sqrt{r}} + \cdots\right\}.$$

For no decay ($\gamma = 0$) effluents discharge, $\Phi = 2$ and the maximum value simplifies to

$$\frac{C_{\max}}{C_{sm}} = 1 - q_2 \left\{ \frac{\varepsilon}{\beta_1 \sqrt{r}} \left(1 - \frac{3L}{\lambda \beta_1^2} \right) + \left(\frac{L}{\lambda \beta_1^2} \right)^2 \cdots \right\}.$$

Figure 8 (right) shows the ratio of maximum concentration $C_{\max}/C_{sm}$ as a function of the discharge rate q_2 when $L = 1$ for three values of $\varepsilon = 1$, 2 and 3. For example, if $\varepsilon = 2$ (or $\varepsilon/\beta_1\sqrt{r} = 0.042$) and both ports are discharging at equal rates $q_2 = q_1 = 0.5$, then the maximum value $C_{\max}$ is about 2.1% less than C_{sm} for no decay effluent ($\gamma = 0$) and about 2.4% for constant decay of $\gamma = 0.0005$ and $\delta = 0$. If the port separation distance $\varepsilon = 3$ (or $\varepsilon/\beta_1\sqrt{r} = 0.063$) and the discharge rate q_2 is increased to 0.75, then the maximum value $C_{\max}$ is decreased by 4.9% for no decay effluent ($\gamma = 0$) and about 5.4% for constant decay of $\gamma = 0.0005$ and $\sigma = 0$. This calculation confirms that installing a two-port diffuser at the end of the outfall pipe will improve the mixing and dilution of the effluent plume in shallow coastal waters [6,7].

7. Concluding Remarks

Analytical solutions have been derived using a two-dimensional decay-advection-diffusion equation in a step seabed depth for modelling the far-field spreading of desalination brine effluents discharge from two outfalls in the coastal waters. The variability of decay of discharged effluents with water depth is accounted for in the solutions. The results show that the long-term impacts of two or more desalination brine outfalls discharging are strongly inter-dependent and compounded from neighbouring outfalls. The human health risk of discharged chemically active effluents from a sufficiently long (effective) outfall is generally considered low. Conversely, a short (ineffective) outfall constitutes a high health risk. Using the maximum value of the compounded concentration at the shoreline, it is found that if two outfalls are independently operated, the maximum value can be kept small as long as the second outfall length is longer than double the first outfall length, and discharging at a rate smaller than the second outfall. If the integrated total effluent discharge load can be shared between two outfalls, then it is found that the maximum value is smaller than that of the single outfall as long as the second outfall length is larger than the first outfall length. A similar result is also found for the case of an outfall with a two-port diffuser installed at the end-of-pipe.

ACKNOWLEDGMENT

This work was supported by the Sultan Qaboos University Internal Grant IG/SCI/DOMS/18/04.

CONFLICT OF INTERESTS

The authors declare that there is no conflict of interests.

REFERENCES

[1] P.J.W. Roberts, H.J. Salas, F.M. Reef, M. Libhaber, A. Labe, J.C. Thomson, Marine Wastewater Outfalls and Treatment Systems, International Water Association (IWA) Publishing, London, 2010.

[2] Institution of Civil Engineers, Long Sea Outfalls, Thomas Telford Ltd. London, 2001.

[3] N. Ahmad, R.E. Baddour, A review of sources, effects, disposal methods, and regulations of brine into marine environments, Ocean Coast. Manage. 87(2014), 1-7.

[4] J.F. Macqueen, R.W. Preston, Cooling water discharges into a sea with a sloping bed, Water Res. 17(1983), 389–395.

[5] D.A. Roberts, E.L. Johnston, N.A. Knott, Impacts of desalination plants discharges on the marine environment: A critical review of published studies, Water Res. 44(2010), 5117-5128.

[6] R. Smith, A. Purnama, Two outfalls in an estuary: Optimal wasteload allocation, J. Eng. Math. 35(1999), 273-283.

[7] A. Purnama, Effluent discharges from two outfalls on a sloping beach, Appl. Math. 5(2014), 3117-3126.

[8] A. Purnama, D.D. Shao, Modeling brine discharge dispersion from two adjacent desalination outfalls in coastal waters, Desalination, 362(2015), 68-73.

[9] S. Lattemann, T. Hopner, Environmental impact and impact assessment of seawater desalination, Desalination, 220(2008), 1-15.

[10] T. Younos, Environmental issues of desalination, J. Contemp. Water Res. Educ. 132(2005), 11-18.

[11] D.J. Gould, D. Munro, Relevance of microbial mortality to outfall design, in Coastal Discharges – Engineering Aspect and Experience, Thomas Telford, Ltd. London, 1981.

[12] P. Mebine, R. Smith, Effects of contaminant decay on the diffusion centre of a river, Environ. Fluid Mech. 6(2006), 101-114.

[13] P. Mebine, R. Smith, Effect of pollutant decay on steady-state concentration distributions in variable depth flow, Environ. Fluid Mech. 9(2009), 573-586.

[14] R. Smith, Effects of non-uniform currents and depth variations upon steady discharges in shallow water, J. Fluid Mech. 110(1981), 373-380.

[15] A. Kay, The effect of cross-stream depth variations upon contaminant dispersion in a vertically well-mixed current, Estuar. Coast. Shelf Sci. 24(1987), 177-204.

[16] D.A. Chin, P.J.W. Roberts, Model of dispersion in coastal waters, J. Hydraul. Eng. 111(1985), 12-28.

[17] I.R. Wood, Asymptotic solutions and behavior of outfall plumes, J. Hydraul. Eng. 119(1993), 553-580.

[18] A. Purnama, H.H. Al-Barwani, T. Bleninger, R.L. Doneker, CORMIX simulations of brine discharges from Barka plants, Oman, Desalin. Water Treat. 32(2011), 329-338.

[19] D.W. Ostendorf, Longshore dispersion over a flat beach, J. Geophys. Res. 87(1982), 4241-4248.

[20] D.L. Craig, H.J. Fallowfield, N.J. Cromar, Comparison of decay rates of faecal indicator organisms in recreational coastal water and sediment, Water Supply, 2(2002), 131-138.

[21] A. Adcroft, R. Hallberg, J.P. Dunne, B.L. Samuels, J.A. Galt, Simulations of underwater plumes of dissolved oil in the Gulf of Mexico, Geophys. Res. Lett. 37(2010), L18605.

[22] V.P. Shukla, Analytical solutions for unsteady transport dispersion of nonconservative pollutant with time-dependent periodic waste discharge concentration, J. Hydraul. Eng. 128(2002), 866-869.

[23] A. Purnama, H.H. Al-Barwani, Spreading of brine waste discharges into the Gulf of Oman, Desalination, 195(2006), 26-31.

[24] H.H. Al-Barwani, A. Purnama, Simulating brine plumes discharged into the seawaters, Desalination, 221(2008), 608-613.